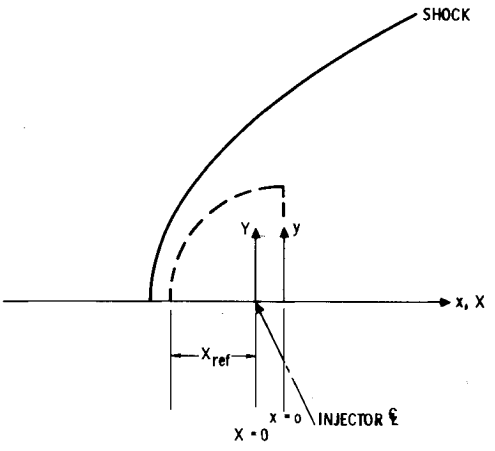

Fig. 1 Geometry for shock shape correlation.

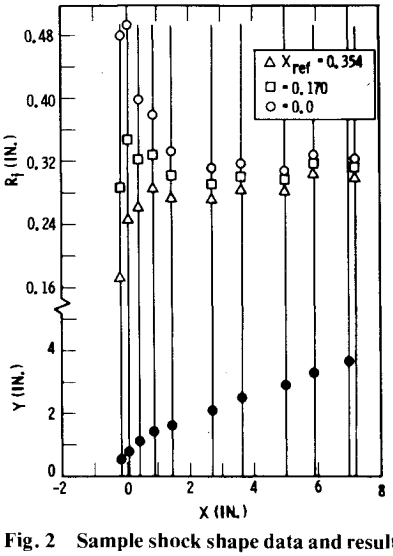

Fig. 2 Sample shock shape data and results.

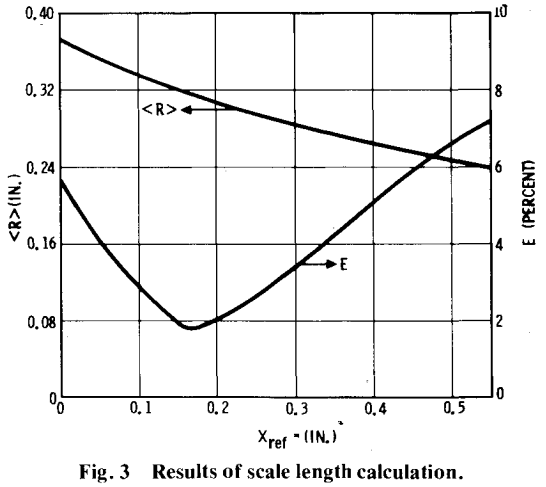

Fig. 3 Results of scale length calculation.

tends to support the shock shape assumption that is the basis of the present method.

Such support can also be found if the errors in the fitting process are small. Figure 3 shows the behavior of rms error E and average scale length $\langle R \rangle$ over part of the range of the values of X_{ref} for which calculations were made, for the same run as the foregoing. The rather sharp minimum shown by E is very satisfactory, and the resulting uncertainty in choice of R (that value of $\langle R \rangle$ for which $E = \min$; here $R = 0.312$) is small. The corresponding value of E is also significantly small, at 1.8%. This is a typical value; the largest value of E among all runs is 5.6%, and the average is 1.9%. No significant difference exists between fuel sources or nozzles. The average value of E over slot nozzle tests, for example, is 1.7%.

These values are small enough to confirm the original assumption that the experimental shock shapes can be well represented by Billig's shock shape expressions.[2] (However, caution should be observed in using the cylinder shock on data from nozzles of transverse aspect ratio less than 10, or using the sphere shock on other than circular nozzles.)

Acknowledgment

This work was done under contract to the U.S. Army Missile Command, Redstone Arsenal, Ala. The Contract Monitor was R. P. Rhoades.

References

[1] Kallis, J. M., "Equivalent Solid Obstacle for Gas Injection into a Supersonic Stream," *AIAA Journal*, Vol. 10, Oct. 1972, pp. 1342-1344.

[2] Billig, F. S., "Shock-Wave Shapes Around Spherical- and Cylindrical-Nosed Bodies," *Journal of Spacecraft and Rockets*, Vol. 4, June 1967, pp. 822-823.

[3] Harvey, D. W., Hopkins, D. F., and Rosen, R., "Experiments on Reacting Gas Jet Penetration," *JANNAF Propulsion Meeting*, Oct. 22-24, 1974, San Diego, Calif.; also *AIAA Journal*, Vol. 15, Jan. 1977, pp. 76-82.

Effect of Surface Roughness on Blunt Body Boundary-Layer Transition

A. J. Laderman*
Aeronutronic Ford Corporation, Newport Beach, Calif.

Nomenclature

D	= model diameter
k	= average height of roughness elements
M	= Mach number
p	= pressure
$Re_{\infty, D}$	$= \rho_\infty u_\infty D/\mu_\infty$
Re_θ	= Reynolds number based on momemtum thickness $= \rho_e u_e \theta/\mu_e$
T	= temperature
u	= velocity
ρ	= density
μ	= viscosity
φ	= angular position of model survey station
Δ	= roughness parameter $kT_e/\theta T_w$
θ	= momentum thickness

Subscripts

e	= boundary-layer edge condition
∞	= freestream condition
w	= wall condition
o	= stagnation condition

Introduction

THIS Note describes the effects of three-dimensional, distributed roughness on boundary-layer transition on a hypersonic blunt body. Although the effects of surface roughness on transition are qualitatively known, relatively little specific information is available in the literature.

Received Oct. 27, 1976; revision received Dec. 3, 1976.

Index categories: Boundary-Layer Stability and Transition; Boundary Layers and Convective Heat Transfer—Laminar.

*Principal Scientist, Fluid Mechanics Section. Member AIAA.

Existing methods or correlations for predicting transition are uncertain. Several studies on the effects of distributed surface roughness have been reported[1-4] but these suffer from several deficiencies. First, while both sand-grain type and uniform, regularly spaced roughness elements were used in these tests, the statistical characteristics of the former were poorly documented, thereby causing large uncertainties in the effective roughness height. Those of the latter have not yet been interpreted in terms of an equivalent sand-grain roughness. Second, most of these tests were conducted under transient cold wall conditions and wall temperatures were estimated rather than determined by measurement. More recently, Anderson[5] reported on a systematic program which overcame most of these objections, although these tests were also carried out under transient, cold wall conditions with local surface heat transfer measurements used to detect transition. Using methods described in Ref. 6, the present data were derived from direct measurement of pitot pressure profiles and hot wire or hot film turbulence surveys across the blunt body boundary layer. The results confirm those of Ref. 5 and, in addition, extend the existing data base to include the adiabatic wall condition and to the region of small roughness height.

Description of Experiment

The experiments were conducted in the 50-in. diam Hypersonic Wind Tunnel B of the Arnold Engineering Development Center. A 14-in. diam porous wall hemisphere flaring into a 5° half-angle cone was operated in continuous flow at $M_\infty = 6$, with stagnation temperature T_o of 390°F and supply pressure P_o ranging from 125 to 280 psia ($2.8\times10^6 < Re_{\infty,D} < 6.2\times10^6$). A selected surface roughness was provided by thin-walled hemispherical shells (or "overlays") fitted over the nosetip.

The flow at position $\varphi > 40°$, where φ is the angle subtended by the intersection of the normal to the surface and the axis of the hemisphere passing through the stagnation point, was surveyed by external probes attached to an overhead actuator. At $\varphi = 10°$, 20°, and 30° the flow was surveyed by probes extended and retracted from inside the model through 0.0035 in. diam holes in its surface. In both instances the actuators mounted either 0.004-0.010-in diam pitot tubes, 0.00002 in. diam hot wire anemometers, or specially constructed thin-film probes. The model was also provided with surface pressure taps, thermocouples, and heat transfer gages in order to monitor the surface conditions. Each type of surface sensor was located on a single ray or element separated by 90°, and extending from the stagnation point to the cone afterbody.

Three roughness overlays, designated Overlays IIIa, IVa and IVb, with "effective" peak to valley roughness heights $k = 4.77$, 2.36, and 1.70 mils, respectively, were used in the experiments (a fourth overlay with $k = 1.44$ mils was tested under adiabatic wall conditions but failed to produce transition). The surface was prepared by coating the overlay with a high temperature paint to act as a binder and then spraying with a selected size of ceramic grit. The surface texture of each overlay was measured at several locations with a profilometer, permitting calculation of the statistical characteristics of the roughness distribution. Typical values of the skewness and flatness factors varied from −0.7 to +0.4 and from 2 to 3.5, respectively, which compares favorably with Gaussian values of 0 and 3.0. The roughness height was determined by numerically averaging the individual roughness elements displayed on the profilometer record and ignoring very small elements which would not contribute to transition and would tend to bias the value of k downward.

The model was cooled by pressurizing the porous dome with cold nitrogen gas supplied by a liquid nitrogen source. The flow coolant was forced through the narrow interface between the dome and overlay before exhausting through several small ports located near the shoulder of the overlay. For the adiabatic wall condition, the coolant flow was shut off. In either case, when thermal equilibrium was attained, the overhead and internal sensors were used to survey the boundary layer and identify the nature of the flow as a function of position on the model.

Results and Discussion

Typical results for Overlay IVa and the adiabatic wall condition are shown in the transition map of Fig. 1 where each $P_o\varphi$ combination for which a survey was made is denoted by either an open, half-filled, or closed symbol denoting laminar, transitional, or tubulent flow, respectively. For this overlay and wall temperature, the transition zone appeared relatively broad and the dashed lines in Fig. 1 depict the start and end of transition. The short vertical lines in Fig. 1 represent the start of transition indicated by the surface temperature measurements. For the remaining overlays, interpretation of the data was more straightforward and transition could be accurately represented by a single line. In all instances, the several survey probes and, for the adiabatic case, the surface thermocouples gave consistent results for transition location. (The latter could not be used as a transition indicator in the cold-wall tests since nonuniformities in the measured surface temperature distribution exceeded the small temperature rise associated with transition from laminar to turbulent flow.) Since the overhead surveys, the internally mounted probes, and the surface sensors were all located along different rays, the consistency of the results implies that transition occurred uniformly around the model as opposed to the "flower petal" pattern that is produced when transition is triggered at isolated locations.

The data for all three overlays are shown in Fig. 2, where they are compared to those of Anderson,[5] who correlated his results in the form

$$Re_\theta \Delta^{0.7} \begin{cases} > 255 \text{ at } M_e = 1 & \text{onset} \quad (1a) \\ = 215 & \text{location} \quad (1b) \end{cases}$$

The onset criterion was derived from the observation by Anderson[5] that transition did not occur on the nosetip beyond the sonic point. The transition parameter on the left-

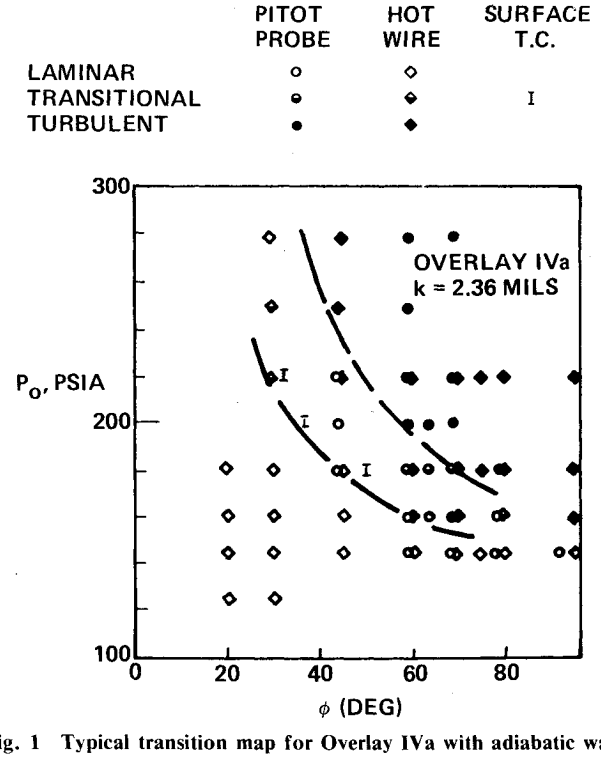

Fig. 1 Typical transition map for Overlay IVa with adiabatic wall temperature.

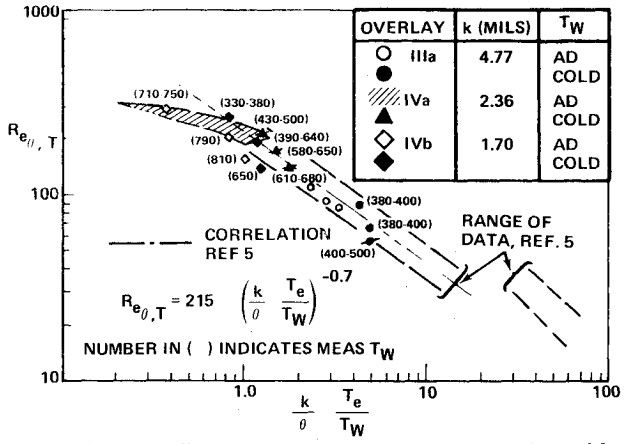

Fig. 2 Rough wall transition results showing comparison with correlation of Ref. 5.

hand side of Eq. (1) can be shown to reach a maximum when $M_e = 1.0$. Consequently, its value at the sonic point must exceed the empirical constant 255 before the transition location is determined as the position where the parameter equals 215. It should be noted that the stagnation point is approached as the value of the right-hand side of Eq. (1b) decreases. The present data are shown as open symbols for the adiabatic case and as filled symbols for the cold-wall condition. In the latter instance, the range of wall temperatures encountered on repeated runs is listed in parenthesies adjacent to the data point and the corresponding uncertainty in the transition coordinates is indicated by the short straight line drawn though the data point. The values of θ used in Fig. 2 were determined from theoretical laminar boundary-layer calculations for a smooth surface. For $\Delta > 1.0$, the agreement between the present results and Anderson's correlation is satisfactory and prompts the following comments. First, although the methods for manufacturing the surface texture differed in the two experiments, the observed agreement implies that the roughness characteristics are quite similar. Second, since the wind-tunnel facilities and the associated noise environment also differed, the agreement between the two experiments further suggests that transition was roughness dominated and that tunnel noise had litte effect on the results. Finally, considering the range of test conditions involved, the test results indicate that Anderson's location correlation is valid for wall temperatures ranging from 0.5 T_o to 1.0 T_o.

For $\Delta < 1.0$, however, the shaded band, representing the transition zone bounded by the dashed curves in Fig. 1, departs from the correlation given by Eq. (1b). These data correspond to transition aft on the nosetip where the onset criterion in Eq. (1a) predicts transition does not occur. The discrepancy may be attributed to differences in the experimental procedures. In the transient tests of Ref. 5 the transition location continuously moved aft during the test and, beyond the sonic point, may have flashed rapidly to the frustum, while for the steady-state condition of the present investigation, transition remained at a fixed location during the test. It is important to note that the trend of the present data for $\Delta < 1.0$ indicates a shift from the roughness-dominated situation (where $\Delta > 1.0$) to the smooth wall region where other effects, such as disturbances in the external stream, may be introduced. This remains an important technical topic whose resolution requires further investigation.

Acknowledgment

Work supported by United States Air Force Space and Missile Systems Organization under Contract F04701-75-C-0232. The contributions of the author's associates, A. Demetriades and L. Von Seggern in planning and executing the experiments are gratefully acknowledged. The author is also indebted to R. Baker, Aerospace Corp., for supplying theoretical calculations of the boundary-layer properties.

References

[1] Deveikis, W. D. and Walker R. W., "Local Aerodynamic Heat Transfer and Boundary Layer Transition on Roughened Sphere-Ellipsoid Bodies at Mach Number 3," NASA TN D-907, Aug. 1961.

[2] Otis, J. H. Jr., Thyson, N., Chen, K. K., Rushton, G., Howey, D., and DiCristina, V., "Strategic Re-entry Technology Program (STREET-A) Final Report, Volume II, Task 7.5, Nosetip Ablation Phenomena," U. S. Air Force, SAMSO TR-70-247, Nov. 1970.

[3] Dunavant, H. C. and Stone, H. W., "Effect of Roughness on Heat Transfer to Hemisphere Cylinders at Mach Numbers 10.4 and 11.4," NASA TN D-3871, March 1967.

[4] Beckwith, I. E. and Gallagher, J. J., "Heat Transfer and Recovery Temperatures on a Sphere with Laminar, Transitional and Turbulent Boundary Layers at Mach Numbers of 2.00 and 4.15," NACA TN-4125, 1957.

[5] Anderson, A. D., "Analysis of PANT Series A Rough Wall Calorimeter Data, Part II: Surface Roughness Effects on Boundary Layer Transition," Aerotherm Div., Acurex Corp. Report No. 73-81.

[6] Demetriades, A., Laderman, A. J., Von Seggern, L., Hopkins, A. T., and Donaldson, J. C., "Effect of Mass Addition on the Boundary Layer of a Hemisphere at Mach 6," *Journal of Spacecrafts and Rockets*, Vol. 13, Aug. 1976, pp 508-509.

Effects of Water Vapor on Thermal Shield Materials

Alfred A. Fote*
The Aerospace Corporation, El Segundo, Calif.

Introduction

THE vulnerability of several flexible thermal control materials to damage under conditions of high humidity was investigated. Deterioration of these materials would destroy their ability to protect spacecraft from excessive heating caused by orbital solar radiation. Exposure to a humid environment could result from failure of an air-conditioning unit at any time prior to launch.

In this study samples of ¼-mil aluminized Mylar, 1-mil aluminized Kapton, and 2-mil silvered Teflon, in the form of squares ½ to 3 in. on a side, were exposed to various controlled humidities and examined for deterioration. The samples were used, as received, without being cleaned or treated. It was discovered that the aluminized Mylar and aluminized Kapton were unaffected by the water vapor; whereas, the silvered Teflon was severely damaged in a few hours.

Effect of Sea-Water Vapor

An artificial sea-water solution was prepared from a standard receipe.[1] One sample of each material was exposed to the vapor of this solution in a sealed container at 24°C for three days. During this time, dry nitrogen was percolated slowly through the solution. The bursting bubbles served to propel the dissolved salts into the vapor,[2] which otherwise would contain only water molecules.

After exposure, each sample was divided in half. One set of samples was exposed to a vacuum for two days. The second set remained in a normal environment for 14 days; then it was also exposed to a vacuum for two days. The reflectivity of the samples in the wavelength region of 1 to 5 μm was measured. This wavelength corresponds to the near-infrared region of the solar spectrum.

Received Dec. 15, 1976.
Index category: Spacecraft Temperature Control.
*Member of the Technical Staff.